



CSIRO

# Measurement of Water and Solute Movement in Large 'Undisturbed' Soil Cores: Analysis of Macknade and Bundaberg Data

Claire M. Cote, Keith L. Bristow, Eva-Jane Ford, Kirsten Verburg and Brian A. Keating

---

CSIRO Land and Water, Townsville  
Technical Report 07/01  
April 2001

ISSN 1446-6171

---



CSIRO LAND and WATER

© 2001 CSIRO To the extent permitted by law, all rights are reserved and no part of this publication covered by copyright may be reproduced or copied in any form or by any means except with the written permission of CSIRO.

**Important Disclaimer:**

CSIRO advises that the information contained in this publication comprises general statements based on scientific research. The reader is advised and needs to be aware that such information may be incomplete or unable to be used in any specific situation. No reliance or actions must therefore be made on that information without seeking prior expert professional, scientific and technical advice. To the extent permitted by law, CSIRO (including its employees and consultants) excludes all liability to any person for any consequences, including but not limited to all losses, damages, costs, expenses and any other compensation, arising directly or indirectly from using this publication (in part or in whole) and any information or material contained in it.

**MEASUREMENT OF WATER AND SOLUTE MOVEMENT IN LARGE  
'UNDISTURBED' SOIL CORES:  
ANALYSIS OF MACKNADE AND BUNDABERG DATA**

Claire Cote<sup>1,2</sup>, Keith L. Bristow<sup>1,2,3</sup>, Eva-Jane Ford<sup>1</sup>, Kirsten Verburg<sup>4</sup>,  
and Brian A. Keating<sup>5,3</sup>

<sup>1</sup>CSIRO Land and Water, PMB Aitkenvale, Townsville, Qld 4814

<sup>2</sup>School of Mathematics, Physics and Computer Science, James Cook University, Townsville  
Qld 4811

<sup>3</sup>CRC for Sustainable Sugar Production, James Cook University, Townsville Qld 4811

<sup>4</sup>CSIRO Land and Water and <sup>5</sup>CSIRO Tropical Agriculture (now CSIRO Sustainable  
Ecosystems), Long Pocket Laboratories, 120 Meiers Road, Indooroopilly, Brisbane Qld 4068

2001 © CSIRO Land and Water

ISSN 1446-6171

Corresponding Author:

Keith L. Bristow  
CSIRO Land and Water  
PMB Aitkenvale  
Townsville, QLD 4814  
Australia

Phone: +61-7-4753 8596

Email: [Keith.Bristow@clw.csiro.au](mailto:Keith.Bristow@clw.csiro.au)

Citation:

Cote, C.M., Bristow, K.L., Ford, E.J., Verburg, K. & B.A. Keating. 2001. Measurement of water and solute movement in large 'undisturbed' soil cores: Analysis of Macknade and Bundaberg data. CSIRO Land and Water Technical Report 07/01, Townsville, Australia.

## TABLE OF CONTENTS

<b>1.</b>	<b>Executive Summary</b> .....	<b>5</b>
<b>2.</b>	<b>Introduction</b> .....	<b>6</b>
<b>3.</b>	<b>Large undisturbed soil core experiments</b> .....	<b>7</b>
3.1.	Outline of Large Core Leaching Facility.....	7
3.2.	Soils and Field Collection of Large Cores .....	7
3.3.	Leaching Experiments .....	8
<b>4.</b>	<b>Solute Transport and the Advection-Dispersion Equation (ADE)</b> .....	<b>9</b>
<b>5.</b>	<b>Analytical Solutions of the ADE</b> .....	<b>11</b>
5.1.	Reduced form of the ADE .....	11
5.2.	Flux-averaged concentrations.....	11
5.3.	Initial condition .....	12
5.4.	Boundary conditions.....	12
5.4.1.	<i>Step application</i> .....	12
5.4.2.	<i>Pulse application</i> .....	12
5.4.3.	<i>Powder application – Dirac Delta Input</i> .....	12
<b>6.</b>	<b>Analysis of Experimental Breakthrough Curves (BTCs) using CXTFIT</b> .....	<b>14</b>
<b>7.</b>	<b>Results and Discussion</b> .....	<b>15</b>
7.1.	Comparison between experimental BTCs and the ADE .....	15
7.2.	Dispersion coefficient.....	15
7.2.1.	<i>Dispersion and pore water velocity</i> .....	15
7.2.2.	<i>Dispersivity</i> .....	16
<b>8.</b>	<b>Summary and Conclusions</b> .....	<b>18</b>
<b>9.</b>	<b>Acknowledgments</b> .....	<b>18</b>
<b>10.</b>	<b>References</b> .....	<b>19</b>
<b>11.</b>	<b>Table captions</b> .....	<b>21</b>
<b>12.</b>	<b>Figure captions</b> .....	<b>21</b>

## 1. Executive Summary

In this report we describe results of leaching experiments carried out on large undisturbed soil cores (300 mm long × 216 mm diameter) obtained from key field sites in Queensland. The soils used in these studies were

- Macknade Alluvial soil (Great Soil Group) or Orthic Tenosol (Australian Classification) obtained from the Macknade Sugar Mill field site near Ingham
- Red Earth (Great Soil Group) or Red Kandosol (Australian Classification) obtained from the Francis farm near Bundaberg
- Red/Yellow Podzolic (Great Soil Group) or Red/Yellow Dermosol (Australian Classification) obtained from the Schulte farm near Bundaberg

Solute breakthrough curves (BTCs) were obtained for these three soils using leaching experiments with three different boundary conditions (BCs)

- (1) constant potential BC where the tracer solution was applied via a disk infiltrometer system,
- (2) fixed potential BC where the tracer solution was applied via a dripper unit, and
- (3) a Dirac delta function BC where the tracer was applied as a surface powder.

In (1) and (2) the tracer could be applied as a step function or as a pulse function. The BTCs obtained from all experiments were analysed with the widely used Advection-Dispersion Equation (ADE) via the CXTFIT programme (Toride et al., 1995) to obtain estimates of the solute transport properties.

We found that the pulse application of solute at the soil surface yielded the most robust dispersion coefficient. We also found that for this experimental condition the dispersivity and the increase in the dispersion coefficient with flow velocity was consistent with results reported in the literature. The “average” dispersivity for these soils and experimental conditions were

- 4 cm for the Tenosol
- 7 cm for the Kandosol, and
- 11 cm for the Dermosol.

These data show that dispersivity increases with stronger soil structure and with the presence of preferential flow paths, such as worm channels.

## 2. Introduction

Fertilisers and other chemicals applied to agricultural lands if not well managed may accumulate in and degrade the soil root zone, or move below the root zone and contaminate underlying groundwater. Attempts to address these issues and improve understanding and management of water and chemicals in the vadose zone has led to development of various models to describe soil water and solute movement. One of the more common approaches currently used is based on the Richards' equation for soil water flow and the Advection-Dispersion Equation (ADE) for solute flow [see for example the LEACHM (Hutson and Wagenet, 1992), HYDRUS-2D (Simunek et al., 1999) and SWIMv2 (Verburg et al., 1997) models]. Successful application of these types of models requires that we have access to appropriate soil water and solute transport properties, and obtaining reliable estimates of the transport properties remains a major challenge. This has led to increased research activity in soil property determinations and a move from making measurements on small repacked cores, to making measurements on large undisturbed cores, and where possible, making in situ measurements in the field.

In an earlier report (Ford et al., 1997) we described a large core leaching facility that has been constructed to facilitate studies on large undisturbed soil cores (roughly 25 cm diameter and 30-60 cm in length), a key aim being to 1) improve understanding of soil water and solute transport processes, and 2) improve our ability to quantify the soil water and solute transport properties. This large core leaching facility is now being used for a range of soil water and solute transport studies. In this report we describe results of leaching experiments carried out on large undisturbed soil cores obtained from key field sites at Ingham (Macknade Sugar Mill farm) and Bundaberg (Schulte and Francis farms). The aim of these leaching experiments was to obtain estimates of the solute transport properties by analysing the solute breakthrough curves (BTCs) obtained under a range of experimental conditions.

The report is structured to provide a brief outline of the large core leaching facility and the soils used in this study, a short description of the solute transport theory as used in the SWIMv2 model, the procedures used to analyse the solute BTCs obtained during the large core leaching experiments, and a general discussion of results.

### **3. Large undisturbed soil core experiments**

#### **3.1. Outline of Large Core Leaching Facility**

The laboratory facility constructed to facilitate leaching studies on large undisturbed soil cores is described in detail by Ford et al. (1997). It was designed to enable application of two different solutions (a background solution and a tracer solution) to large soil cores at different or equal rates, one after the other, with minimal mixing of solutions at the changeover. The system allows solution leaching from the base of the cores to be collected at known time intervals to provide breakthrough data of the tracer solution. It is the analysis of these data that provides information on the soils solute transport properties. The apparatus was designed and manufactured to enable simultaneous measurement on four large soil cores and to allow the system to run unattended for lengthy periods.

There are options for three different ways of applying water and solutions to the large soil cores and several methods of controlling lower boundary conditions. The upper boundary conditions can be set as a surface pond, or controlled using a disc infiltrometer (so that the suction at the surface is fixed) or drip infiltrometer (to simulate fixed intensity rainfall). Lower boundary conditions can be set as free drainage (seepage boundary condition) or controlled at a particular suction. If needed, a powder form of the tracer chemical can be applied to the soil surface prior to applying the background solution. This can be used to simulate field application of solid fertilisers and chemicals.

#### **3.2. Soils and Field Collection of Large Cores**

The main soils used in these studies included a

1. Macknade Alluvial soil (Great Soil Group) or Orthic Tenosol (Australian Classification) obtained from the Macknade Sugar Mill field site near Ingham. This soil had a particle size distribution of 59.5% sand, 20.8% silt, 19.6% clay, and bulk density of  $1.51 \text{ Mg m}^{-3}$
2. Red Earth (Great Soil Group) or Red Kandosol (Australian Classification) obtained from the Francis farm near Bundaberg. This soil had a particle size distribution of 60.6% sand, 15.4% silt, 24.1% clay, and a bulk density of  $1.62 \text{ Mg m}^{-3}$
3. Red/Yellow Podzolic (Great Soil Group) or Red/Yellow Dermosol (Australian Classification) obtained from the Schulte farm near Bundaberg. This soil had a particle size distribution of 74.3% sand, 16.3% silt, 9.4% clay, and a bulk density of  $1.70 \text{ Mg m}^{-3}$

We also used repacked sand known as Sandfly Creek Sand as a reference for some of our runs. This sand had a particle size distribution of 98% sand, 1% silt, 1% clay, and packed to a bulk density of  $1.52 \text{ Mg m}^{-3}$ .

Large undisturbed soil cores were collected from the above mentioned field sites using 236 mm ID PVC sewer pipe cut to a length of 30 cm. At Macknade the field cores were collected using the plain PVC pipe with an outer bevel at the lower edge to facilitate insertion of the core. It was inserted directly into the soil by 'bashing' a steel plate, positioned across the top of the ring, with a sledge hammer. The core was then excavated by hand and any gaps between the soil and inner surface of the core filled with melted petroleum jelly.

Sampling at Bundaberg was done with the same PVC sewer pipe but with a reinforced cutting edge as described by McKenzie and Jacquier (1996). This inner reinforcing ring is made of a short length of sewer pipe with a small segment removed to allow it to fit inside the main core. The outside edge is also bevelled to provide a cutting edge. When taking the soil core the inner ring creates an air filled annulus that allows a sealant to be used to ensure good contact between the soil and core and thereby minimises any edge flow down the core. In addition to the reinforcing ring, two slots were cut into the core prior to field sampling. These slots were for buriable TDR probe access. They were 60 by 20 mm in size and located 80 mm from the top and bottom of the core. Removable plugs were inserted in the slots prior to prevent petroleum jelly from escaping. Core diameter measurements were based on a petroleum jelly thickness of 10 mm, instead of 7 mm, due to partial absorption of the jelly into the soil core. This gave an effective diameter of 216 mm for these field cores.

Field cores were collected by first digging a circular trench around an intact 'pillar' of undisturbed soil which was taller than and had a slightly larger diameter than the core. The core was then pushed into the pillar of soil, allowing the edges of the pillar to fall away from the core as it was inserted. Following complete insertion the core was excavated by hand. The air gap between the soil and inner surface of the core was then filled with melted petroleum jelly.

After collection, the large field cores were transported to Townsville and stored in a cold room (6-8°C) until they were required for use in the laboratory.

### **3.3. *Leaching Experiments***

The large cores were brought from cold storage to the leaching laboratory as needed. The cores were prepared for particular runs as described by Ford et al. (1997). A summary of all runs carried out and the associated experimental conditions are given in Table 1 and Table 2. They divide into 3 main groupings:

1. tracer solution applied via the disk infiltrometer system; Runs M1 to M7
2. tracer solution applied via the dripper unit; Runs B1 to B5
3. tracer applied as a surface powder; Runs B6 to B9

Prior to Run B1 the sand cores were wet with distilled water until saturated and then allowed to drain overnight before the experiment began. This was an attempt to minimise 'fingering' which may occur in sands. Prior to Runs B4 and B6 the sand cores were saturated with 0.025 Molar  $K_2SO_4$  followed by 1 litre of soil wetting agent (1 ml/l) applied to the surface. This was then flushed through with 0.025 Molar  $K_2SO_4$  overnight prior to starting the experimental runs.

The first run for the surface applied powder (Run B6) was carried out without wetting the cores or establishing steady state flow conditions with the background solution. Prior to applying the bromide powder for this run a fan was used to blow air across the core surfaces for 3 days to dry them as much as possible. The bromide powder was then applied to the surface after which the background solution was applied. In the other three runs, Runs B7, B8 and B9, the soil cores were wet and brought to steady state flow conditions with the background solution before bromide powder was applied. In these cases the flow obviously had to be stopped to apply the powder but this was done in as short a time as practically possible.

#### 4. Solute Transport and the Advection-Dispersion Equation (ADE)

There are two key processes that govern solute transport in soils and these are diffusion, where ions move in the soil water in response to concentration gradients, and advection (or convection), where ions move with the soil water. Note that in the soils literature convection and advection are often used interchangeably to describe the same process. Differences in pore water velocities within individual pores and between pores of different sizes lead to an additional effect known as hydrodynamic dispersion, which results in a spreading of solute as the solute moves with the soil water. Because both diffusion and hydrodynamic dispersion result in reduced solute concentration gradients they are often combined in the mathematical description of solute transport, and referred to as the ‘dispersion coefficient’ as discussed below.

The dispersion and advection processes are captured in SWIMv2 by means of the Advection-Dispersion Equation (ADE) (Verburg et al., 1997)

$$\frac{\partial \theta c}{\partial t} + \frac{\partial \rho s}{\partial t} = \frac{\partial}{\partial z} \left( \theta D \frac{\partial c}{\partial z} \right) - \frac{\partial qc}{\partial z} + \phi \quad (1)$$

where

- $c$  = solute concentration in solution (mol or g solutes  $\text{cm}^{-3}$  water)
- $s$  = adsorbed concentration (mol  $\text{g}^{-1}$  soil or g  $\text{g}^{-1}$  soil)
- $\rho$  = soil bulk density ( $\text{g cm}^{-3}$ )
- $t$  = time (h)
- $z$  = depth (cm)
- $\theta$  = water content ( $\text{cm}^3 \text{cm}^{-3}$ )
- $D$  = dispersion coefficient which is the combined hydrodynamic dispersion and diffusion coefficient ( $\text{cm}^2 \text{h}^{-1}$ )
- $q$  = water flux density ( $\text{cm h}^{-1}$ )
- $\phi$  = source/sink term (mol  $\text{cm}^{-3} \text{h}^{-1}$  or g  $\text{cm}^{-3} \text{h}^{-1}$ )

The first term on the RHS describes the diffusion and dispersion processes while the second term describes the convective process.

The ‘dispersion coefficient’  $D$  is expected to vary with the mean flow velocity. A simple functional relationship is often assumed, of the form

$$D = \tau D_o + \varepsilon v^n \quad (2)$$

where

- $\tau$  = tortuosity factor (-)
- $D_o$  = ionic or molecular diffusion coefficient in free water ( $\text{cm}^2 \text{h}^{-1}$ )
- $\varepsilon$  = dispersivity of the medium ( $(\text{cm}^2 \text{h}^{-1})/(\text{cm h}^{-1})^n$ )
- $v$  = pore water velocity = the ratio of the area-averaged water flux  $q$  to the water content  $\theta$ , i.e.  $v = q/\theta$  ( $\text{cm h}^{-1}$ )

$n$  = empirical constant (-)

Tortuosity is described as

$$\tau = a(\theta - b)^\xi \quad (3)$$

where

$a$  = empirical constant (-)

$b$  = empirical constant (-)

$\xi$  = empirical constant (-)

This equation for tortuosity is general and allows flexible parameterisation. It is, for example, able to handle the commonly used relationship of Millington and Quirk (1961)

$$\theta = \theta^{10/3} / \theta_s^2 \quad (4)$$

where  $\theta_s$  is the saturated water content ( $\text{cm}^3 \text{cm}^{-3}$ ).

Exchange of solutes between the soil solution and soil itself is governed by the Freundlich exchange isotherm expressed as

$$s = k c^\eta \quad (5)$$

where

$k$  = coefficient of Freundlich isotherm ((mol or g adsorbed solute  $\text{g}^{-1}$  soil)/(mol or g solute  $\text{cm}^{-3}$  water) $^\eta$ )

$\eta$  = power of Freundlich isotherm (-)

If  $\eta = 1$ , Eq.(5) reduces to a linear isotherm.

At present SWIMv2 deals with only one solute at a time. The choice of units for solute concentration,  $c$ , is flexible, and any units can be used as long as they are expressed in an amount  $\text{cm}^{-3}$  soil. Units of  $s$ ,  $\phi$ , and  $k$  change accordingly.

Values for the diffusion coefficient  $D_o$  can be found in several literature sources (e.g., Robinson and Stokes, 1965; Lehrman, 1979; Weast and Astle, 1980; Kemper, 1986; Sadeghi et al., 1988). Some values for common ions from Kemper (1986) in the units required by SWIMv2 ( $\text{cm}^2 \text{h}^{-1}$ ) are (at 25°C)  $\text{Br}^- = 0.074$ ;  $\text{NO}_3^- = 0.068$ ;  $\text{Cl}^- = 0.073$ ;  $\text{K}^+ = 0.071$ ;  $\text{Na}^+ = 0.048$ ;  $\text{Mg}^{2+} = 0.026$ ;  $\text{H}^+ = 0.335$ . Note that in most cases solutes move as ion pairs so care is needed in determining the 'correct'  $D_o$  for the particular problem at hand.

In this report we focus on determination of the dispersion coefficient  $D$  and because we use  $\text{Br}^-$  (which is not adsorbed strongly by the soil particles in soils with low anion exchange capacities) as the tracer, we do not concern ourselves here with the exchange isotherms.

## 5. Analytical Solutions of the ADE

The ADE (Eq.(1)) is the general equation governing solute transport in soils. Successful solution of this ADE requires specification of the initial conditions (ICs), boundary conditions (BCs), source/sink terms, and the system properties. It's solution yields the solute concentrations as a function of time and depth together with the solute flux densities. The ADE is usually solved numerically and there are only a few special cases for which analytical solutions exist.

### 5.1. *Reduced form of the ADE*

If one can assume that

- the soil properties within the soil core are uniform with depth
- there is steady flow of water through the soil core
- there is a uniform water content within the soil core
- the solute being studied is non-reactive, and
- there is no sink or source for the solute

then the ADE can be written in reduced form as

$$\frac{\partial C}{\partial T} = \frac{1}{P} \frac{\partial^2 C}{\partial Z^2} - \frac{\partial C}{\partial Z} \quad (6)$$

where

- $C$  =  $c/c_o$  with  $c_o$  a characteristic concentration (i.e. the initial solute concentration in the soil, or the concentration of the solution applied to the soil)
- $T$  =  $v t / L$  with  $L$  a characteristic length (i.e. the length of the soil column). This dimensionless variable is referred to as pore volume, as it represents the amount of water that has passed through the soil relative to the total amount of water present in the soil.
- $Z$  =  $z / L$
- $P$  =  $v L / D$ , referred to as the Péclet number.

### 5.2. *Flux-averaged concentrations*

In many solute transport studies, the experimental conditions are such that the measured concentrations are flux-averaged rather than volume-averaged (for instance, when, as is the case for our breakthrough experiments, we measure the concentration in samples of an effluent solution). To interpret such measurements, these concentrations are not assumed to represent resident concentrations ( $C$ ) at the outflow boundary, but they are treated as flux-averaged concentrations, referred to as  $C_f$ , and defined by

$$C_f = C - \frac{D}{v} \frac{\partial C}{\partial z} \quad (7)$$

The flux-averaged concentration represents the amount of solutes per unit volume of fluid passing through a given cross-section during an elementary time interval. One can show that when  $C$  obeys Eq.(6),  $C_f$  obeys this equation as well (see e.g. Parker and van Genuchten (1984)).

### 5.3. *Initial condition*

For all breakthrough experiments, the initial tracer concentration in the soil cores was 0, and the initial condition can then be written as

$$C = 0; \quad T = 0, \quad 0 \leq Z \leq 1 \quad (8)$$

### 5.4. *Boundary conditions*

#### 5.4.1. *Step application*

A step application refers to an abrupt change in solution concentration at the soil surface (Runs M1 to M7). The boundary condition at the top of the column is

$$C - \frac{1}{P} \frac{\partial C}{\partial Z} = C_f = 1; \quad 0 < T, \quad Z = 0 \quad (9)$$

In this case, the characteristic concentration  $c_o$  is the constant concentration of the tracer solution being applied. The boundary condition at the base of the column is

$$\frac{\partial C}{\partial Z} = 0; \quad 0 < T, \quad Z = 1 \quad (10)$$

#### 5.4.2. *Pulse application*

For a pulse application (Runs B1 to B5), the tracer solution is applied at the soil surface for a finite duration  $T_o$ . The boundary condition at the top of the column is

$$C - \frac{1}{P} \frac{\partial C}{\partial Z} = C_f = 1; \quad 0 < T \leq T_o, \quad Z = 0 \quad (11)$$

In this case as well the characteristic concentration  $c_o$  is the constant concentration of the tracer solution being applied. The boundary condition at the base of the column is the same as for the step application (Eq.(10)).

#### 5.4.3. *Powder application – Dirac Delta Input*

Assuming the solute dissolves instantaneously, the application of solute in powder form at the soil surface (Runs B6 to B9) can be approximated as an instantaneous solute application (Jury and Roth, 1990) with the following boundary condition

$$C - \frac{1}{P} \frac{\partial C}{\partial Z} = C_f = C_o(T); \quad 0 < T \leq T_o, Z = 0 \quad (12)$$

$$C_o(T) = M_o \delta(T)$$

where  $\delta$  is a Dirac delta function with respect to  $T$  and  $M_o$  is the dimensionless amount of applied solute. A dimensional Dirac input is given by

$$c_o(t) = \frac{m}{q A} \delta(t) \quad (13)$$

where  $m$  (g) is the total mass of solute applied to the soil and  $A$  (cm<sup>2</sup>) is the cross-sectional area of the soil core. In this case, the characteristic concentration  $c_o$  is equal to

$$c_o = \frac{m}{q A} \quad (14)$$

The dimensional and dimensionless Dirac inlet conditions are related via

$$\delta(T) = \frac{v}{L} \delta(t) \quad (15)$$

which gives

$$c_o(T) = \frac{v}{L} \frac{m}{q A} \delta(T), \quad \text{and} \quad (16)$$

$$\frac{c_o(T)}{c_o} = C_o(T) = \frac{v}{L} \delta(T)$$

which yields

$$M_o = \frac{v}{L} \quad (17)$$

Toride et al. (1995) give the analytical solutions of the ADE for the above initial and boundary conditions. These analytical expressions are not reproduced here as they are relatively complicated.

## 6. Analysis of Experimental Breakthrough Curves (BTCs) using CXTFIT

To analyse experimental breakthrough data obtained using the large undisturbed soil cores, the CXTFIT programme (Toride et al., 1995) can be used to estimate the solute transport parameters using a non-linear least-squares parameter optimisation method. This approach allows the unknown parameter  $D$  in the ADE (Eq.(1) and (6)) to be determined by fitting the appropriate analytical solution of the ADE to experimental results. We present here the main ideas and concepts underlying CXTFIT. More detailed information about the programme can be found in Toride et al. (1995).

Data analysis using CXTFIT requires

- a choice of initial condition (Eq.(8))
- a choice of boundary condition (in our case, step, pulse or Dirac delta input), and the parameters associated with the boundary condition ( $T_o$  for a pulse,  $M_o$  for a Dirac delta input)
- the value of the input parameters ( $v$ ,  $L$ )
- the experimental data, i.e. the values of  $C$  as a function of  $T$  at  $Z = 1$  (concentration in the effluent solution)

The programme then gives the value of the fitted parameter  $D$ , the calculated values of  $C$  as a function of  $T$  at  $Z = 1$  so that experimental and theoretical BTCs can be plotted and compared, and the results of the non-linear least-squares analysis. Only the data analysis carried out on the undisturbed field soil cores is presented here.

## 7. Results and Discussion

### 7.1. Comparison between experimental BTCs and the ADE

The experimental BTCs as compared with the ADE (Eq.(6)) are shown in Fig. 1 for the Tenosol with pulse and step input, in Fig. 2 for the Kandosol with pulse input, in Fig. 3 and Fig. 4 for the Kandosol with Dirac delta input, and in Fig. 5 for the Dermosol with pulse input. The programme CXTFIT yielded the dispersion coefficient  $D$  which is given in Table 3 for all BTCs carried out with the Tenosol, in Table 4 for all BTCs carried out with the Kandosol, and in Table 5 for all BTCs carried out with the Dermosol. These tables also give the input parameters required by CXTFIT, the  $R^2$  value for regression of the observed BTCs versus the fitted BTCs, and the derived Péclet number.

For the step and pulse top boundary condition, the ADE provides an adequate description of the experimental results. The theoretical model fits the experimental data very well except for the Tenosol BTC 7 (Run M7) for which the  $R^2$  value is only 0.10, and for the Dermosol 2 BTC 2 (Run D5) for which the  $R^2$  value is 0.68. For all the other runs the  $R^2$  values ranged from 0.95 to 0.99 for the step boundary condition, and from 0.81 to 0.99 for the pulse boundary condition.

The ADE does not describe the experimental BTCs very well for the Dirac delta input. For the Kandosol 4 BTC 1 (Run D6) the  $R^2$  value is 0.12. For all the other experiments it ranges from 0.72 to 0.97. To derive an analytical solution of the ADE that would describe experimental BTCs with application of solute in powder form at the soil surface, we had to assume the solute would dissolve instantaneously in the applied water, and that the boundary condition could be approximated as an instantaneous solute application. In reality, not all the powder would dissolve instantaneously and this could explain at least some of the discrepancy between the experimental and theoretical results. Whilst application of solute in powder form at the soil surface reproduces more closely field application of fertilisers, it is probably not the best method to use for the purpose of determining the soils solute transport parameters.

For the Tenosol, solution was applied via the disk infiltrometer. For the Kandosol and Dermosol with pulse boundary conditions at the surface, solution was applied via the dripper unit. The data analysis and  $R^2$  values do not indicate any obvious differences between these two methods of solute application. Both solution application methods yielded robust results when used in conjunction with the pulse boundary condition.

### 7.2. Dispersion coefficient

#### 7.2.1. Dispersion and pore water velocity

The values of the dispersion coefficient  $D$  (Eq.(2)) obtained with CXTFIT are given in Table 3, Table 4, and Table 5. Typical values for  $D$  as determined in this study are 5 to 70 cm<sup>2</sup>/hr. Typical values for the molecular diffusion coefficient in free water  $D_o$  are usually around 10<sup>-1</sup> cm<sup>2</sup>/hr, and the tortuosity factor is less than 1. In this case,  $\tau D_o$  can therefore be neglected when compared with  $\varepsilon v^n$ , which yields a simple linear relationship

$$\ln D = n \ln v + \ln \varepsilon \quad (18)$$

where  $\ln$  gives the natural logarithm. The parameters  $n$  and  $\varepsilon$  can then be estimated by fitting a straight line to a  $\ln$ - $\ln$  plot of the dispersion coefficient as a function of the pore water velocity. These plots and the fitted lines are shown in Fig. 6. Note that Runs M7 and D6 were not described well by the ADE and they have been excluded from this analysis. The slope and intersect of the fitted lines yield the value of  $n$  and  $\varepsilon$ , and these values are given in Table 6.

For the pulse top boundary condition, Eq.(18) describes well the relationship between  $D$  and  $v$  with a  $R^2$  value of 0.88 for the Tenosol, 0.93 for the Kandosol and 0.53 for the Dermosol. Our dispersivity values are  $\varepsilon = 1.83$  for the Tenosol, 1.94 for the Kandosol, and 3.13 for the Dermosol. Typical dispersivities obtained from previously published undisturbed soil core experiments range from 0.64 cm to 190 cm with most values between 2 cm and 10 cm (Table 7). The values of  $\varepsilon$  obtained with Eq.(18) are well within the range of dispersivity values published in the literature. However, for most values in Table 7, it was assumed that  $n = 1$ , as recommended by Sposito et al. (1986). Our data also suggest that this is a reasonably valid assumption as our  $n$  values range from 1.03 to 1.28. In the next section we show the dispersivity values obtained when assuming  $n = 1$ .

For the step top boundary condition and powder application, Eq.(18) does not adequately describe the relationship between  $D$  and  $v$  ( $R^2 = 0.03$  for the Tenosol step application, and  $R^2 = 0.131$  for the Kandosol powder application). In the case of the powder application, the ADE did not describe the experimental data very well, so it is not surprising that we do not obtain a consistent relationship between  $D$  and  $v$ . In the case of the step application, the ADE described the experimental data very well. However,  $D$  is determined using a non-linear least-squares optimisation technique, which is weighted towards the rising limb of the BTC because the sum of the squared deviations to be minimised is taken in the vertical direction (Brusseau et al., 1989). In the step application,  $D$  is determined by data points on the rising limb, while in the pulse application  $D$  is determined by data points from both the rising and descending limbs. Hence, the determination of  $D$  is more robust for the pulse application than for the step application because there are more data points against which the optimisation technique is weighted. This could explain why the pulse application yields a more consistent relationship between  $D$  and  $v$  than the step application.

### 7.2.2. Dispersivity

The dispersivity of different soils are more easily compared if the empirical constant  $n$  is assumed to be 1. With such an assumption, Eq.(18) gives a linear relationship between  $D$  and  $v$  and the dispersivity can be calculated as

$$\varepsilon = D/v \quad (19)$$

The ratio  $D/v$  (which is the dispersivity) calculated for our data is given in Table 3, Table 4, and Table 5. Dispersivity calculated using Eq.(19) is shown for each experiment in Fig. 7.

For the Tenosol, Run M7 clearly yields a dispersivity much higher than that obtained for the other runs ( $\varepsilon = 34.3$  cm for Run M7 compared with  $2.0 \leq \varepsilon \leq 5.4$  for all the other runs). It was noted in the previous section that the ADE did not describe Run M7 very well and that this run could be excluded from this analysis. By doing so, the average dispersivity obtained for

the Tenosol is  $4.1 \pm 1.3$  cm (Table 8). We can also calculate the average dispersivity obtained for the Tenosol when using the step boundary condition only, which is  $4.0 \pm 1.8$  cm. The average dispersivity obtained for the Tenosol when using the pulse boundary condition only is  $4.2 \pm 0.1$  cm. It is apparent from this that the choice of boundary condition did not influence the calculation of the ratio  $D/\nu$  as much as it influenced the determination of the parameter  $n$ . The standard error of the dispersivity is quite low and we can conclude that the value of the dispersivity for this Tenosol and for our experimental conditions is around 4 cm ( $4.2 \pm 0.1$  cm).

For the Kandosol, all  $\varepsilon$  values are below 10 cm except for Runs 9B, 9D and 3D. There is no particular reason to exclude these runs from this analysis as they were well described by the ADE (see  $R^2$  values in Table 4). The only thing we can note is that Run 9B was the last experiment carried out on Kandosol 2, Run 9D was the last experiment carried out on Kandosol 4, and Run 3D was the last experiment carried out on Kandosol 3. Structural changes with time could be one reason that affected the dispersivity. If we include Runs 9B, 9D and 3D in the analysis, we obtain an average dispersivity of  $7.8 \pm 4.8$  cm for all Runs,  $9.5 \pm 5.1$  cm for the Runs with pulse boundary condition only, and  $6.6 \pm 4.2$  cm for the Runs with a Dirac boundary condition only (Table 8). If we exclude Runs 9B, 9D and 3D from the analysis, we obtain an average dispersivity of  $5.7 \pm 2.1$  cm for all Runs,  $7.4 \pm 1.7$  cm for the Runs with the pulse boundary condition only, and  $4.2 \pm 1.1$  cm for the Runs with the Dirac boundary condition only (Table 8). Excluding Runs 9B, 9D and 3D dramatically reduces the experimental variation in the dispersivity. We saw in the previous section that the pulse boundary condition yielded more robust values of the dispersion coefficient than the Dirac boundary condition, and conclude that the value of the dispersivity for this Kandosol is around 7 cm ( $7.4 \pm 1.7$  cm).

For the Dermosol, Run 5D clearly yields a dispersivity value much higher than that obtained for the other runs ( $\varepsilon = 29$  cm for Run 5D compared with  $8.6 \leq \varepsilon \leq 12.3$  for all the other runs). As with the Kandosol, Run 5D was the last experiment carried out on Dermosol 2, and it is possible that structural changes may also have occurred in this soil. If we include Run 5D, we obtain an average dispersivity of  $15.3 \pm 8.0$  cm, but if we exclude Run 5D, we obtain an average dispersivity of  $10.7 \pm 1.6$  cm (Table 8). We conclude that the value of the dispersivity for this Dermosol is roughly 11 cm ( $10.7 \pm 1.6$  cm).

The dispersivity  $\varepsilon$  is usually accepted as a characteristic of the porous medium of interest. Many studies have shown however that the dispersivity of undisturbed soil cores can be much greater than that of columns filled with the same soil, but sieved and repacked (e.g. Cassel et al., 1974; Starret et al., 1996). Soil structure can therefore greatly influence the dispersivity. The study of Verburg et al. (2001) provides a detailed pedological description of the soils used in this study. It shows that the Tenosol had a weak structure (dispersivity  $\approx 4$ cm) and that the Kandosol was characterised by a moderate 2-5 mm polyhedral structure (dispersivity  $\approx 7$ cm). Dispersivity clearly increased with soil structure as shown by Starret et al.(1996). The Dermosol was characterised as massive but containing worm channels and the dispersivity for this soil ( $\approx 11$  cm) was greater than for the two previous soils. These data highlight the effect of structure and/or macropores on dispersivity, and on solute transport in general. Our data therefore shows that dispersivity increases with stronger structure and with the presence of preferential flow paths, such as worm channels.

## 8. Summary and Conclusions

This reports summarises results of leaching experiments carried out on large undisturbed soil cores obtained from key field sites at Ingham (Macknade Sugar Mill) and Bundaberg (Schulte and Francis farms). The soils studied were a Tenosol, Kandosol, and Dermosol, providing us with a range of soil textures and structures. The aim of these leaching experiments was to determine the dispersion coefficient  $D$  by comparing the solute breakthrough curves (BTCs) obtained under a range of experimental conditions with analytical solutions of the ADE, using the programme CXTFIT.

We found that the experimental condition that yielded the most robust dispersion coefficient involved a pulse application of solute. It is recommended that for the purpose of determining the solute transport parameters, this method be used. We also found that for this experimental condition, the dispersivity and the relationship between the dispersion coefficient and flow velocity was, in general, consistent with those found in the literature. The data show that the dispersivity increased with stronger structure and with the presence of preferential flow paths, such as worm channels (dispersivity was roughly equal to 4 cm for the Tenosol, 7 cm for the Kansosol and 11 cm for the Dermosol).

Dispersivity is a necessary input parameter for the various models such as HYDRUS-2D and SWIMv2 that describe soil water and solute movement. We provide measured data for three soils in this report, but caution against inappropriate use of these data. Additional studies are needed to determine the general applicability of these results, to help build a more complete data base and greater understanding of dispersivity across a wider range of soils and flow conditions.

## 9. Acknowledgments

Thanks to Vic Catchpoole for his assistance in collecting field cores.

This work was supported by the CSIRO Division of Soils (now CSIRO Land and Water), Sugar Research and Development Corporation, Land and Water Research and Development Corporation and the James Cook University Collaborative Grants Program.

Thanks to Peter Ross for his continued interest and input to this work.

## 10. References

- Anamosa, P. R., P. Nkedi-Kizza, W. G. Blue, and J. B. Sartain. 1990. Water movement through an aggregated, gravelly Oxisol from Cameroon . *Geoderma* 46:263-281.
- Beven, K. J., D. E. Henderson, and A. D. Reeves. 1993. Dispersion parameters for undisturbed partially saturated soil. *J. Hydrology* 143:19-43.
- Brusseau, M. L., P. S. C. Rao, R.E. Jessup, and J. M. Davidson. 1989. Flow interruption: a method for investigating sorption non equilibrium. *J. Contam. Hydrol.* 4:223-240.
- Cassel, D. K., T. H. Krueger, F. W. Schroer, and E. B. Norum. 1974. Solute movement through disturbed and undisturbed soil cores. *Soil Sci. Soc. Am. Proc.* 38:36-40.
- Dyson, J. S. and R. E. White. 1987. A comparison of the convection-dispersion equation and transfer function model for predicting chloride leaching through an undisturbed, structured clay soil . *J. Soil Sci.* 38:157-172.
- Ford, E.J., K.L. Bristow, K. Verburg, B.A. Keating, and K. R .J. Smettem. 1997. Measurement of water and solute movement in large 'undisturbed' soil cores: Experimental facility. *CSIRO Land and Water Technical Report* 11/1997.
- Gupte, S. M., D. E. Radcliffe, D. H. Franklin, L. T. West, E. W. Tollner, and P. F. Hendrix. 1996. Anion transport in a Piedmont Ultisol: II. Local-Scale Parameters. *Soil Sci. Soc. Am. J.* 60:762-770.
- Henderson, D. E., A. D. Reeves, K. J. Beven, and N. A. Chappell. 1996. Flow separation in undisturbed soil using multiple anionic tracers. Part 2. Steady-state core-scale rainfall and return flows and determination of dispersion parameters. *Hydrological processes* 10:1451-1465.
- Hutson, J.L. and R.J. Wagenet. 1992. LEACHM - Leaching Estimation and Chemistry Model, Version 3: User Manual. Cornell University, Ithaca, New York 14853, USA.
- Jury, W. A. and K. Roth. 1990. Transfer Functions and Solute Movement Through Soil. Birkhauser, Basel.
- Kemper, W.D. 1986. Solute diffusivity, pp. 1007-1024, In *Methods of soil analysis, Part I. Physical and mineralogical method*. Agronomy Monograph No.9 (2<sup>nd</sup> ed.), Agronomy Society of America - Soil Science Society of America, Madison, Wisconsin.
- Lehrman, A. 1979. Geochemical processes, Wiley-Interscience, New York.
- Mallants, D., M. Vanclooster, and J. Feyen. 1996. Transect study on solute transport in a macroporous soil. *Hydrological processes* 10:55-70.
- Millington, R.J. and R.H Stokes. 1965. Electrolyte solutions, Butterworths, London.
- Parker, J. C. and M. Th. van Genuchten. 1984. Flux-averaged and volume-averaged concentrations in continuum approaches to solute transport. *Water. Resour. Res.* 20:866-872.
- Persson, M. and R. Berndtsson. 1999. Water application frequency effects on steady-state solute transport parameters. *J. Hydrology* 225:140-154.
- Sadeghi, A.M., D. E. Kissel, and M. L Cabrera. 1988. Temperature effects on urea diffusion coefficients and urea movement in soil, *Soil Sci. Soc. Am. J.* 52: 46-49.

- Seyfried, M. S. and P. S. C. Rao. 1987. Solute transport in undisturbed columns of an aggregated tropical soil: preferential flow effects. *Soil Sci. Soc. Am. J.* 51:1434-1444.
- Simunek, J., M. Sejna, and M. Th. van Genuchten. 1999. HYDRUS-2D / MESHGEN-2D: Simulating water flow and solute transport in two-dimensional variably saturated media . International Groundwater Modeling Centre, Colorado School of Mines, Golden, Colorado. IGWMC - TPS 53C.
- Smettem, K. R. J. 1984. Soil water residence time and solute uptake 3. Mass transfer under simulated winter rainfall conditions in undisturbed soil cores. *J. Hydrology* 67:235-248.
- Sposito, G., W. A. Jury, and V. K. Gupta. 1986. Fundamental problems in the stochastic convection-dispersion model of solute transport in aquifers and field soils . *Water Resour. Res.* 22:77-88.
- Starret, S. K., N. E. Christians, and T. A. Austin. 1996. Comparing dispersivities and soil chloride concentrations of turfgrass-covered undisturbed and disturbed soil columns. *J. Hydrology* 180:21-29.
- Toride, N., F. J. Leij, and M. Th. van Genuchten. 1995. The CXTFIT code for estimating transport parameters from laboratory or field tracer experiments, Version 2.1 . *U.S. Salinity Laboratory, Riverside, California* Research Report No.137.
- Vanclooster, M., D. Mallants, J. Vanderborght, J. Diels, J. van Orshoven, and J. Feyen. 1995. Monitoring solute transport in a multi-layered sandy lysimeter using Time Domain Reflectometry. *Soil Sci. Soc. Am. J.* 59:337-344.
- Verburg, K., Bridge, B.J., Bristow, K.L. & B.A. Keating. 2001. Properties of selected soils in the Gooburrum – Moore Park area of Bundaberg. CSIRO Land and Water Technical Report 09/2001, Canberra, Australia. ISBN 0 643 06092 8, pp. 77.
- Verburg, K., P. J. Ross, and K.L. Bristow. 1997. SWIMv2.1 User Manual. *CSIRO Division of Soils Divisional Report* No. 130.
- Vogeler, I., D. R. Scotter, S. R. Green, and B. E. Clothier. 1997. Solute movement through undisturbed soil columns under pasture during unsaturated flow. *Aust. J. Soil Res.* 35:1153-1163.
- Weast, R.C., and M.J. Astle (Eds). 1980. CRC Handbook of chemistry and physics, 60<sup>th</sup> ed., CRC Press, Boca Raton, Florida.
- Wierenga, P. J. and M. Th. van Genuchten. 1989. Solute transport through small and large undisturbed soil columns. *Ground Water* 27:35-42.

## 11. Table captions

- Table 1: Summary of leaching studies carried out on large soil cores obtained from the Macknade field site near Ingham (Tenosol).
- Table 2: Summary of leaching studies carried out on large soil cores obtained from the Francis (Kandosol) and Schulte (Dermosol) field sites near Bundaberg
- Table 3: CXTFIT results for the Tenosol soil. Here,  $v$  is the pore water velocity,  $T_o$  is the dimensionless pulse duration,  $D$  is the fitted dispersion coefficient,  $R^2$  is the coefficient of determination,  $\varepsilon$  is the dispersivity and  $Pé$  is the Péclet number.
- Table 4: CXTFIT results for the Kandosol soil. Here,  $v$  is the pore water velocity,  $T_o$  is the dimensionless pulse duration,  $M_o$  is the dimensionless amount of applied solute,  $D$  is the fitted dispersion coefficient,  $R^2$  is the coefficient of determination,  $\varepsilon$  is the dispersivity and  $Pé$  is the Péclet number.
- Table 5: CXTFIT results for the Dermosol soil. Here,  $v$  is the pore water velocity,  $T_o$  is the dimensionless pulse duration,  $D$  is the fitted dispersion coefficient,  $R^2$  is the coefficient of determination,  $\varepsilon$  is the dispersivity and  $Pé$  is the Péclet number.
- Table 6: Values of the parameters  $n$  and dispersivity  $\varepsilon$  which characterise the functional relationship between the flow velocity and the dispersion coefficient (Eq.(2)).
- Table 7: Representative values of dispersivity for undisturbed soil cores obtained from the literature.
- Table 8: Average dispersivity calculated as the ratio of  $D / v$  for each soil.

## 12. Figure captions

- Fig. 1: Comparison between experimentally determined BTCs and the Advection-Dispersion Equation (ADE) for the Tenosol (Macknade).
- Fig. 2: Comparison between experimentally determined BTCs with pulse input and the Advection-Dispersion Equation (ADE) for the Kandosol (Francis).
- Fig. 3: Comparison between experimentally determined BTCs with Dirac delta input and the Advection-Dispersion Equation (ADE) for the Kandosol (Francis).
- Fig. 4: Comparison between experimentally determined BTCs with Dirac delta input and the Advection-Dispersion Equation (ADE) for the Kandosol (continued).
- Fig. 5: Comparison between experimentally determined BTCs with pulse input and the Advection-Dispersion Equation (ADE) for the Dermosol (Schulte).
- Fig. 6: Log-Log plots of the dispersion coefficient as a function of the flow velocity, with the fitted linear relationship.
- Fig. 7: Dispersivity  $\varepsilon$  (defined as  $D/v$ ) for each run carried out on the three soils.

**Table 1: Summary of leaching studies carried out on large soil cores obtained from the Macknade field site near Ingham (Tenosol).**

Run #	Identification for core #A,B,C,D and lower boundary conditions applied				Upper boundary condition	Function applied	Chemical application method		Average application rate (mm/h)
	A	B	C	D			Background	Tracer	
M1			Block 13 Rep 2 Seepage		Disc infil. (10 mm tension)	Step	0.025 Molar K <sub>2</sub> SO <sub>4</sub>	0.05 Molar KBr	9 (Increasing during run)
M2			Block 13 Rep 2 Seepage		Disc infil. (10 mm tension)	Step	0.025 Molar K <sub>2</sub> SO <sub>4</sub>	0.05 Molar KBr	9 (Increasing during run)
M3			Block 13 Rep 2 Seepage		Disc infil. (10 mm tension)	Pulse	0.025 Molar K <sub>2</sub> SO <sub>4</sub>	0.05 Molar KBr	11 (Increasing during run)
M4			Block 13 Rep 2 Seepage		Disc infil. (40 mm tension)	Step	0.025 Molar K <sub>2</sub> SO <sub>4</sub>	0.05 Molar KBr	6 (Increasing during run)
M5			Block 13 Rep 2 Seepage		Disc infil. (40 mm tension)	Pulse	0.025 Molar K <sub>2</sub> SO <sub>4</sub>	0.05 Molar KBr	7 (Increasing during run)
M6			Block 13 Rep 2 Seepage		Disc infil. (80 mm tension)	Step	0.025 Molar K <sub>2</sub> SO <sub>4</sub>	0.05 Molar KBr	4 (Steady during run)
M7			Block 13 Rep 2 Seepage		Disc infil. (80 mm tension)	Pulse	0.025 Molar K <sub>2</sub> SO <sub>4</sub>	0.05 Molar KBr	2 (Decreasing during run)

**Table 2: Summary of leaching studeis carried out on large soil cores obtained from the Francis (Kandosol) and Schulte (Dermosol) field sites near Bundaberg**

Run #	Identification for core #A,B,C,D and lower boundary conditions applied				Upper boundary condition	Function applied	Chemical application method		Average application rate (mm/h)
	A	B	C	D			Background	Tracer	
B1	SFCS No Wick	Kandosol 1 (Fra 1) No Wick	SFCS With Wick	Kandosol 3 (Fra 4) With Wick	Drip infiltrrometer	Pulse	0.025 Molar K <sub>2</sub> SO <sub>4</sub>	0.05 Molar KBr	12
B2	SFCS No Wick	Kandosol 1 (Fra 1) No Wick	SFCS With Wick	Kandosol 3 (Fra 4) With Wick	Drip infiltrrometer	Pulse	0.025 Molar K <sub>2</sub> SO <sub>4</sub>	0.05 Molar KBr	16
B3	SFCS No Wick	Kandosol 1 (Fra 1) No Wick	SFCS With Wick	Kandosol 3 (Fra 4) With Wick	Drip infiltrrometer	Pulse	0.025 Molar K <sub>2</sub> SO <sub>4</sub>	0.05 Molar KBr	4
B4	SFCS No Wick	Dermosol 1 (Sch 7) No Wick	SFCS With Wick	Dermosol 2 (Sch 12) With Wick	Drip infiltrrometer	Pulse	0.025 Molar K <sub>2</sub> SO <sub>4</sub>	0.05 Molar KBr	4 (Cores B and D with 1 cm head)
B5	SFCS No Wick	Dermosol 1 (Sch 7) No Wick	SFCS With Wick	Dermosol 2 (Sch 12) With Wick	Drip infiltrrometer	Pulse	0.025 Molar K <sub>2</sub> SO <sub>4</sub>	0.05 Molar KBr	16 (Cores B and D with 10 cm head)

**Table 2 (continued): Summary of leaching studeis carried out on large soil cores obtained from the Francis (Kandosol) and Schulte (Dermosol) field sites near Bundaberg**

Run #	Identification for core # A,B,C,D and lower boundary conditions applied				Upper boundary condition	Function applied	Chemical application method		Average application rate (mm/h)
	A	B	C	D			Background	Tracer	
B6	SFCS Sand bed at 20 cm suction	Kandosol 2 (Fra 5) Sand bed at 20 cm suction	SFCS Sand bed at 20 cm suction	Kandosol 4 (Fra 6) Sand bed at 20 cm suction	Drip infiltrrometer	Dirac (Powder)	0.025 Molar K <sub>2</sub> SO <sub>4</sub>	Granular KBr. A & B Strip. C & D Surface. Surface initially dry	16
B7	SFCS Sand bed at 20 cm suction	Kandosol 2 (Fra 5) Sand bed at 20 cm suction	SFCS Sand bed at 20 cm suction	Kandosol 4 (Fra 6) Sand bed at 20 cm suction	Drip infiltrrometer	Dirac (Powder)	0.025 Molar K <sub>2</sub> SO <sub>4</sub>	Granular KBr. A & B Strip. C & D Surface. Surface initially wet	16
B8	SFCS Sand bed at 20 cm suction	Kandosol 2 (Fra 5) Sand bed at 20 cm suction	SFCS Sand bed at 20 cm suction	Kandosol 4 (Fra 6) Sand bed at 20 cm suction	Drip infiltrrometer	Dirac (Powder)	0.025 Molar K <sub>2</sub> SO <sub>4</sub>	Granular KBr. A & B Strip. C & D Surface. Surface initially wet	16
B9	SFCS Sand bed at 20 cm suction	Kandosol 2 (Fra 5) Sand bed at 20 cm suction	SFCS Sand bed at 20 cm suction	Kandosol 4 (Fra 6) Sand bed at 20 cm suction	Drip infiltrrometer	Dirac (Powder)	0.025 Molar K <sub>2</sub> SO <sub>4</sub>	Granular KBr. A & B Strip. C & D Surface. Surface initially wet	12

NB. SFCS = Sand Fly Creek sand

Fra = Francis field soil (Kandosol)  
Sch = Schulte field soil (Dermosol)  
n/a = not applicable

**Table 3: CXTFIT results for the Tenosol soil. Here,  $v$  is the pore water velocity,  $T_o$  is the dimensionless pulse duration,  $D$  is the fitted dispersion coefficient,  $R^2$  is the coefficient of determination,  $\epsilon$  is the dispersivity and  $Pé$  is the Péclet number.**

Run #	Soil core	BTC Rep	Top BC	Input Parameters		Fitted Parameter	Derived parameters		
				$v$ (cm/hr)	$T_o$	$D$ (cm <sup>2</sup> /hr)	$R^2$	$\epsilon$ ( $D/v$ )	$Pé$
M2	Tenosol	2	Step	3.25	N/A	6.6	0.95	2.0	14.8
M3	Tenosol	3	Pulse	2.76	0.737	11.52	0.99	4.2	7.2
M4	Tenosol	4	Step	2.28	N/A	10.50	0.99	4.6	6.5
M5	Tenosol	5	Pulse	2.28	0.569	9.80	0.81	4.3	7.0
M6	Tenosol	6	Step	1.21	N/A	6.58	0.95	5.4	5.5
M7	Tenosol	7	Pulse	0.61	0.502	20.90	0.10	34.3	0.9

**Table 4: CXTFIT results for the Kandosol soil. Here,  $v$  is the pore water velocity,  $T_o$  is the dimensionless pulse duration,  $M_o$  is the dimensionless amount of applied solute,  $D$  is the fitted dispersion coefficient,  $R^2$  is the coefficient of determination,  $\varepsilon$  is the dispersivity and  $Pé$  is the Péclet number.**

				Input Parameters		Fitted Parameter	Derived parameters		
Run #	Soil core	BTC Rep	Top BC	$v$ (cm/hr)	$T_o$ for Pulse $M_o$ for Dirac	$D$ (cm <sup>2</sup> /hr)	$R^2$	$\varepsilon$ ( $D / v$ )	$Pé$
B1	Kandosol 1	1	Pulse	4.94	1.657	50.82	0.99	10.3	2.9
B2	Kandosol 1	2	Pulse	7.05	1.326	55.36	0.87	7.9	3.8
B3	Kandosol 1	3	Pulse	2.03	1.765	41.37	0.96	5.6	1.5
B6	Kandosol 2	1	Dirac	7.18	0.239	26.56	0.78	3.7	8.1
B7	Kandosol 2	2	Dirac	7.26	0.242	26.88	0.72	3.7	8.1
B8	Kandosol 2	3	Dirac	4.46	0.149	23.51	0.86	5.3	5.7
B9	Kandosol 2	4	Dirac	5.00	0.167	70.58	0.92	14.1	2.1
D1	Kandosol 3	1	Pulse	4.59	1.544	33.31	0.97	7.3	4.1
D2	Kandosol 3	2	Pulse	6.70	1.271	41.37	0.96	6.2	4.9
D3	Kandosol 3	3	Pulse	2.02	1.741	10.5	0.97	5.2	5.8
D6	Kandosol 4	1	Dirac	6.18	0.206	26.56	0.12	4.3	7.0
D7	Kandosol 4	2	Dirac	6.50	0.217	16.54	0.72	2.5	11.8
D8	Kandosol 4	3	Dirac	4.43	0.148	26.19	0.85	5.9	5.1
D9	Kandosol 4	4	Dirac	4.90	0.163	63.75	0.97	13.0	2.3

**Table 5: CXTFIT results for the Dermosol soil. Here,  $v$  is the pore water velocity,  $T_o$  is the dimensionless pulse duration,  $D$  is the fitted dispersion coefficient,  $R^2$  is the coefficient of determination,  $\epsilon$  is the dispersivity and  $Pé$  is the Péclet number.**

Run #	Soil core	BTC Rep	Top BC	Input Parameters		Fitted Parameter	Derived parameters		
				$v$ (cm/hr)	$T_o$	$D$ (cm <sup>2</sup> /hr)	$R^2$	$\epsilon$ ( $D / v$ )	$Pé$
B4	Dermosol 1	1	Pulse	0.53	1.703	4.58	0.98	8.6	14.8
B5	Dermosol 1	2	Pulse	1.38	1.718	15.60	0.99	11.3	7.2
D4	Dermosol 2	1	Pulse	0.39	1.208	4.77	0.94	12.3	6.5
D5	Dermosol 2	2	Pulse	0.68	0.863	19.60	0.68	29.0	7.0

**Table 6: Values of the parameters  $n$  and dispersivity  $\varepsilon$  which characterise the functional relationship between the flow velocity and the dispersion coefficient (Eq.(2)).**

Soil core	Top BC	$n$	$\varepsilon$ ( $\text{cm}^{2-n} \text{hr}^{1-n}$ )	$R^2$
Tenosol	Pulse	1.18	1.83	0.88
Tenosol	Step	0.08	2.34	0.03
Kandosol	Pulse	1.28	1.94	0.93
Kandosol	Dirac	-0.89	8.71	0.13
Dermosol	Pulse	1.03	3.13	0.53

**Table 7: Representative values of dispersivity for undisturbed soil cores obtained from the literature.**

<b>Study</b>	<b>Core dimensions</b>	<b>Dispersivity (cm)</b>
Anamosa et al. (1990)	Diameter: 9.6 cm Length: 80 cm	3.3 ( $n=1.3$ )
Dyson and White (1987)	Diameter: 22 cm Length: 16 cm	2.9 – 13.9
Gupte et al. (1996)	Diameter: 15 cm Length: 33 – 64 cm	$6.6 \pm 2.6$
Henderson et al. (1996)	Diameter: 30.5 cm Length: 35 - 56 cm	6.9 – 190
Mallants et al. (1996)	Diameter: 20 cm Length: 20 cm	7.4
Persson and Berndtsson (1999)	Diameter: 30 cm Length: 65 cm	1.3 – 3.5
Seyfried and Rao (1987)	Diameter: 11 cm Length: 30 cm	2.4 – 6.7
Smettem (1984)	Area: 300 cm <sup>2</sup> Length: 25 cm	1.3 – 21.8
Starret et al. (1996)	Diameter: 10 cm Length: 20 cm	9.4 – 27.6
Vanclooster et al. (1995)	Diameter: 80 cm Length: 100 cm	4 – 8
Vogeler et al. (1997)	Diameter: 30 cm Length: 30 cm	7
Wierenga and van Genuchten (1989)	Diameter: 5.1 cm Length: 30 cm	0.64 – 0.84
	Diameter: 194.5 cm Length: 600 cm	5.5

**Table 8: Average dispersivity calculated as the ratio of  $D / \nu$  for each soil.**

		<b>Average Dispersivity (Standard deviation)</b>
<b>Tenosol</b>	All Runs (excluding M7)	4.1 (0.3)
	Runs with Step BC only	4.0 (1.8)
	Runs with Pulse BC only	4.2 (0.1)
<b>Kandosol</b>	All Runs	7.8 (4.8)
	Runs with Pulse BC only	9.5 (5.1)
	Runs with Dirac BC only	6.6 (4.2)
	All Runs, excluding 9B, 9D, 3B	5.7 (2.1)
	Runs with Pulse BC only, excluding 3B	7.4 (1.7)
	Runs with Dirac BC only, excluding 9B, 9D	4.2 (1.1)
<b>Dermosol</b>	All Runs	15.3 (8)
	All Runs, excluding 5D	10.7 (1.6)

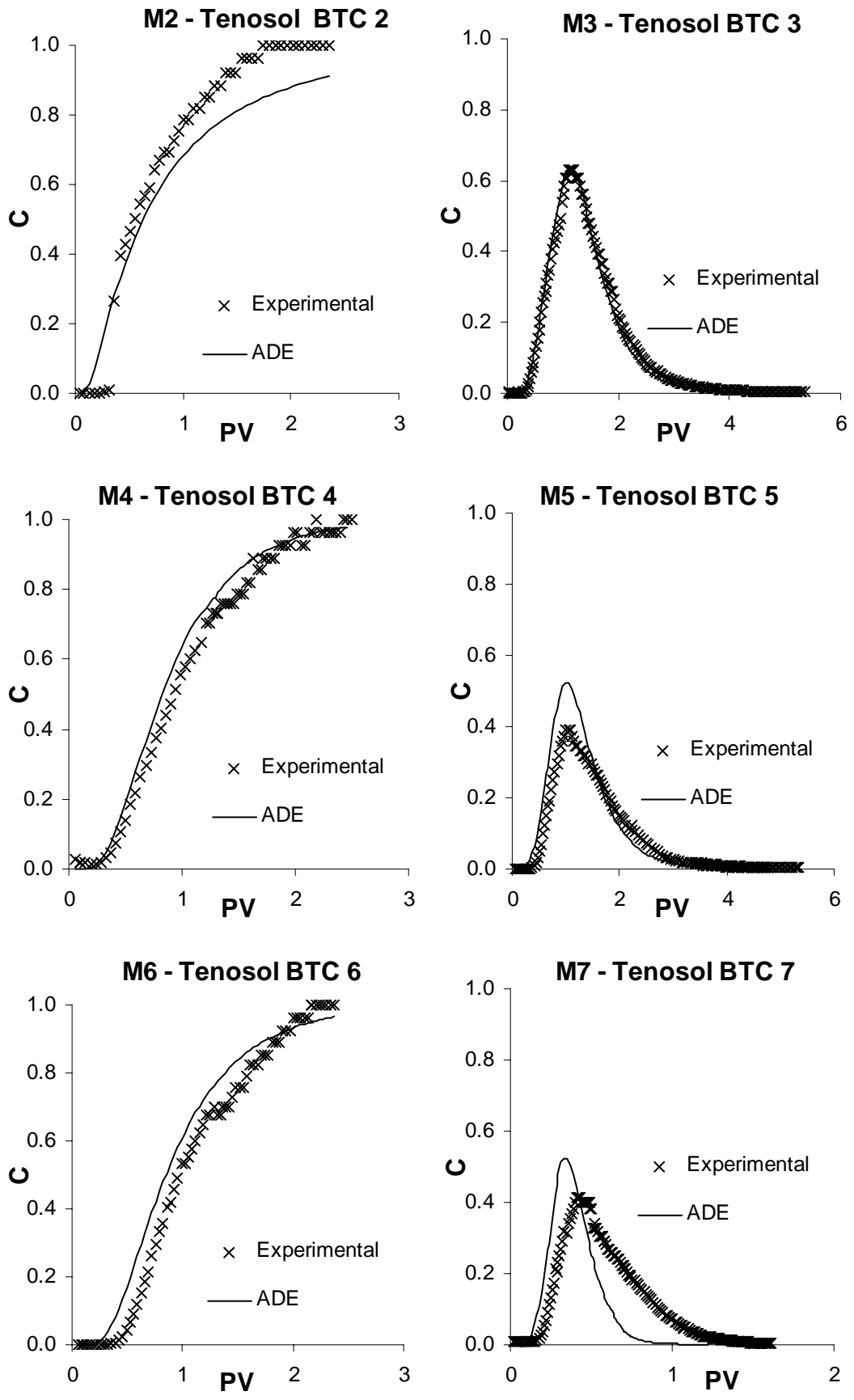


**Fig. 1: Comparison between experimentally determined BTCs and the Advection-Dispersion Equation (ADE) for the Tenosol (Macknade).**

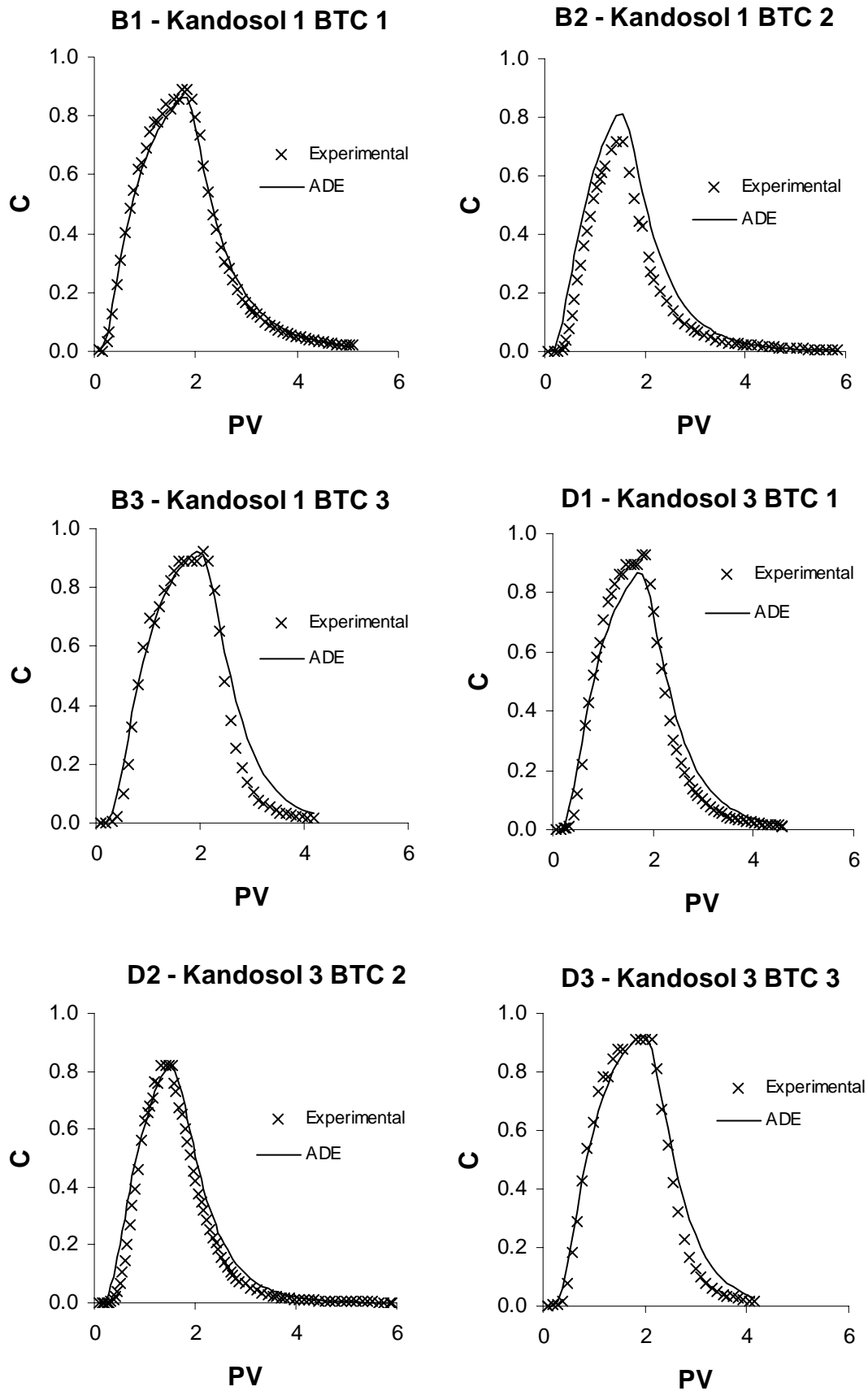


**Fig. 2: Comparison between experimentally determined BTCs with pulse input and the Advection-Dispersion Equation (ADE) for the Kandosol (Francis).**

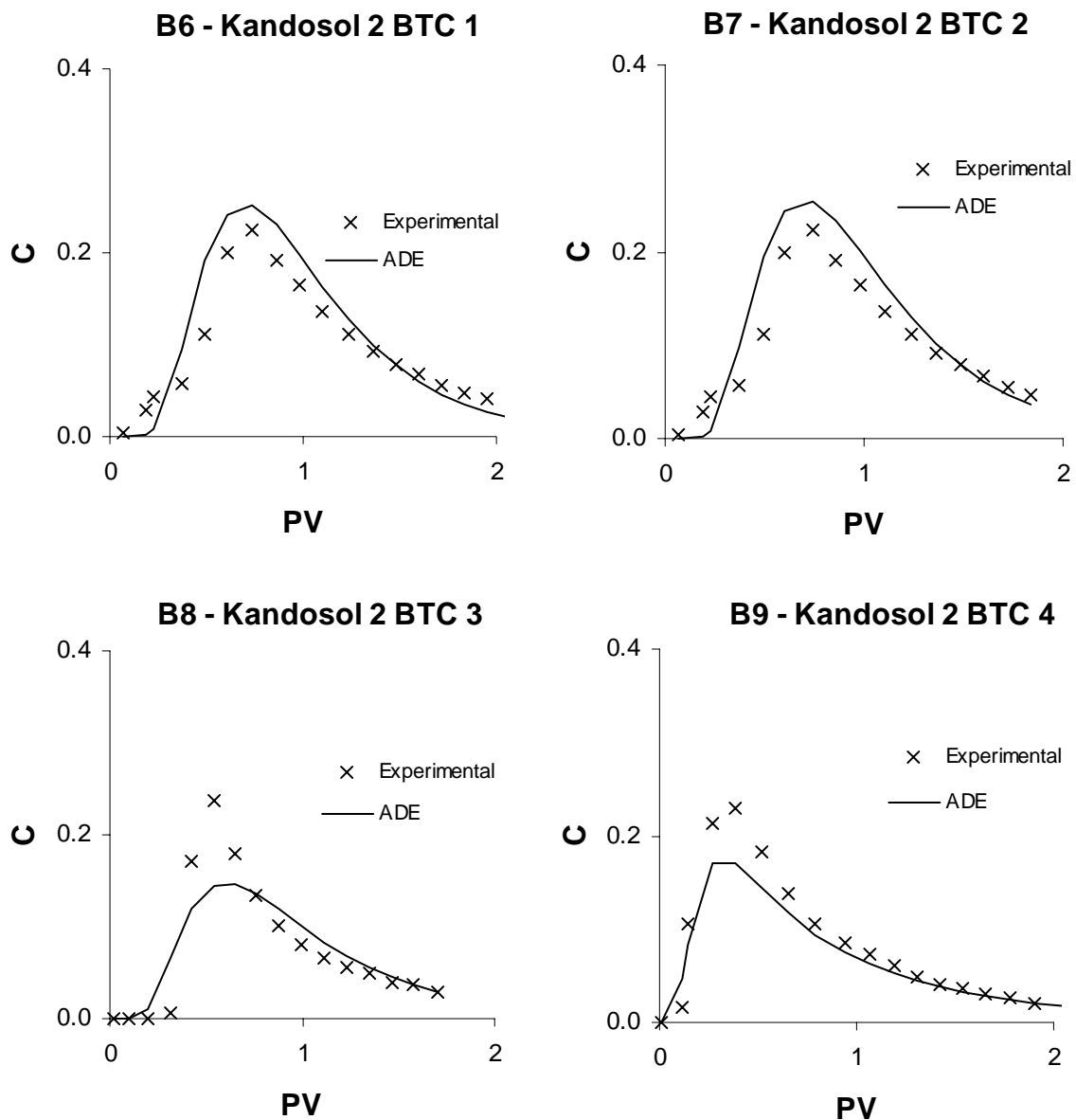


**Fig. 3: Comparison between experimentally determined BTCs with Dirac delta input and the Advection-Dispersion Equation (ADE) for the Kandosol (Francis).**

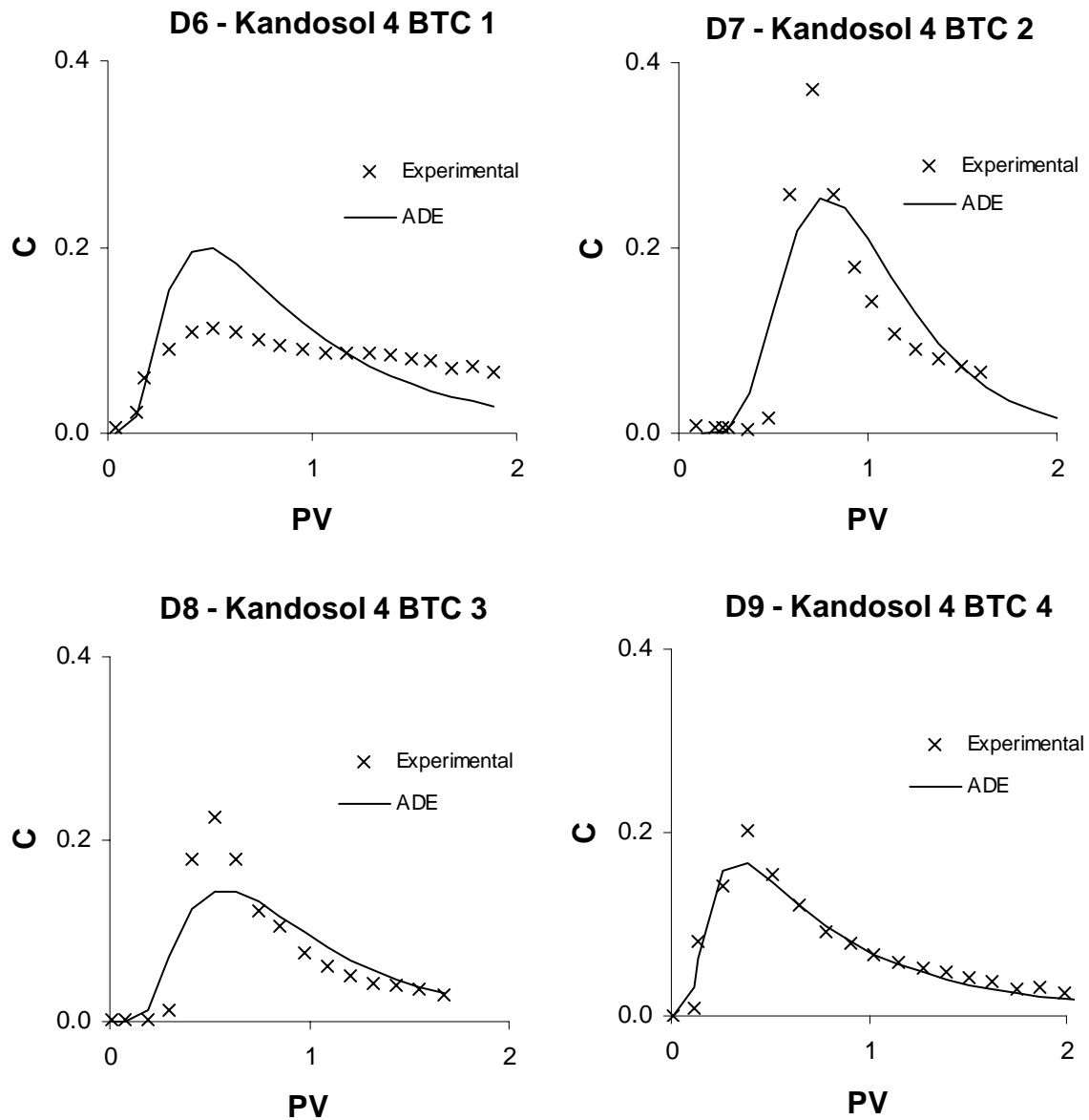


**Fig. 4: Comparison between experimentally determined BTCs with Dirac delta input and the Advection-Dispersion Equation (ADE) for the Kandosol (continued).**

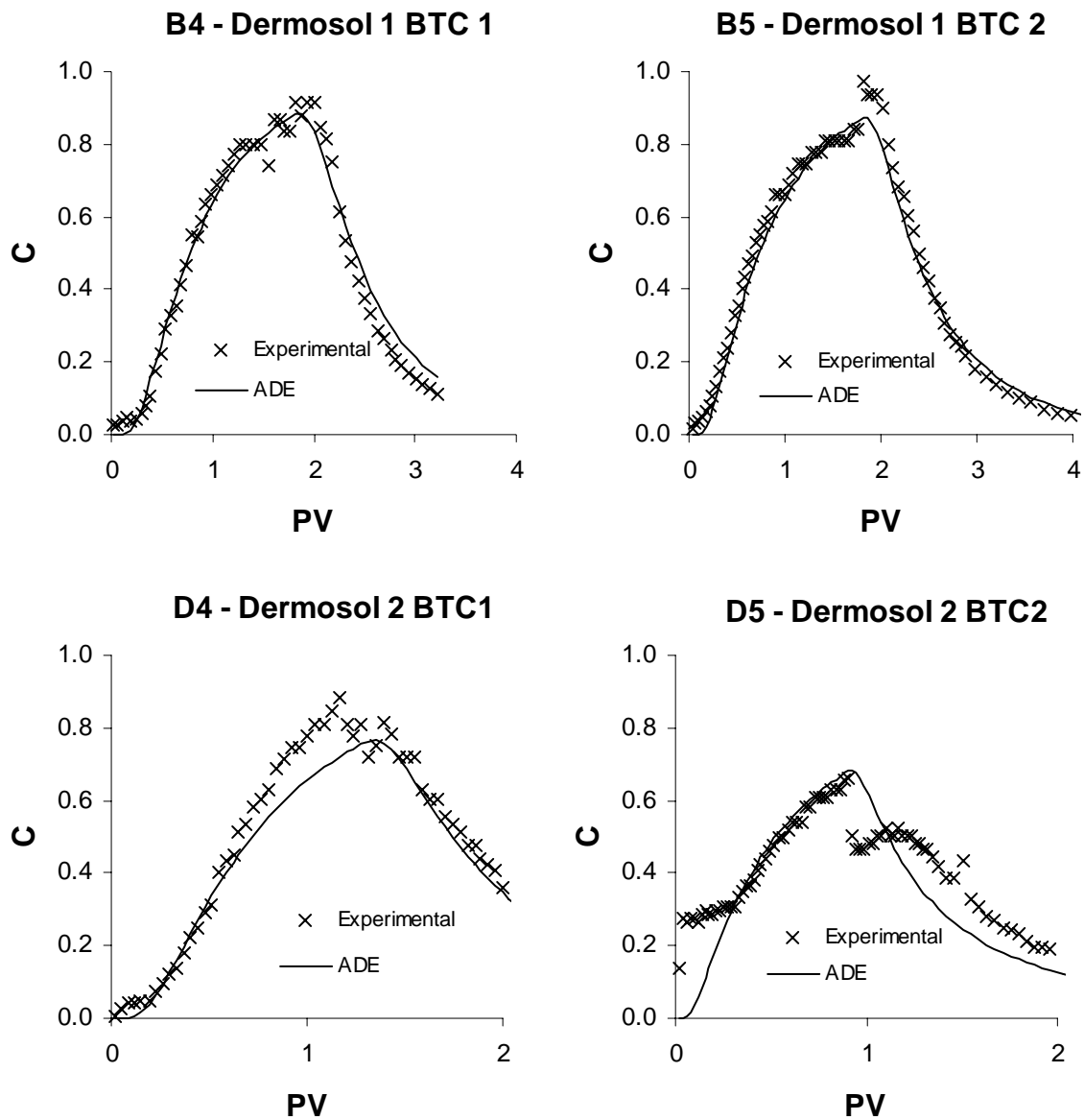
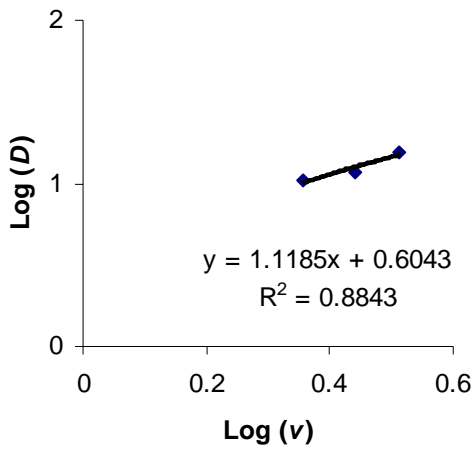
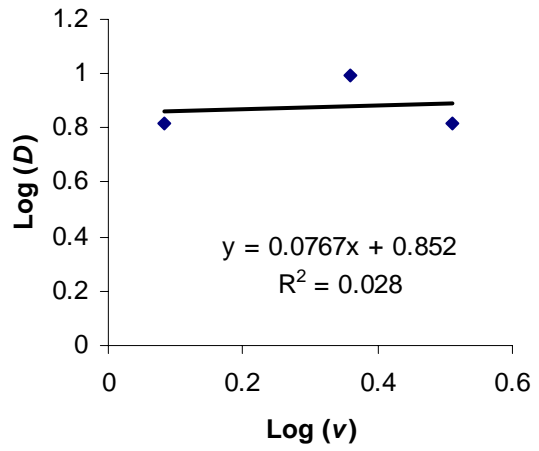


**Fig. 5: Comparison between experimentally determined BTCs with pulse input and the Advection-Dispersion Equation (ADE) for the Dermosol (Schulte).**

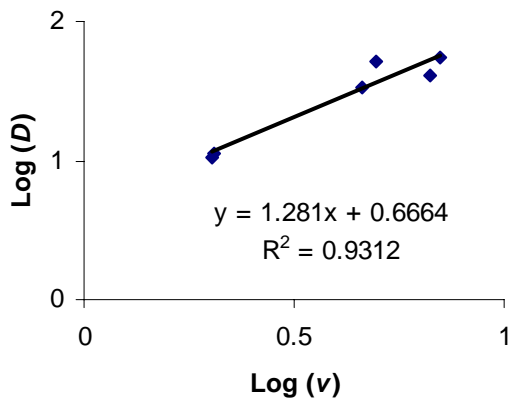
**Tenosol - Pulse Application**



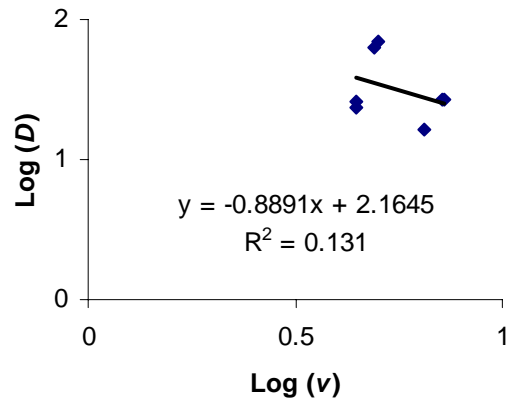
**Tenosol - Step Application**



**Kandosol - Pulse Application**



**Kandosol - Dirac Application**



**Dermosol - Pulse Application**

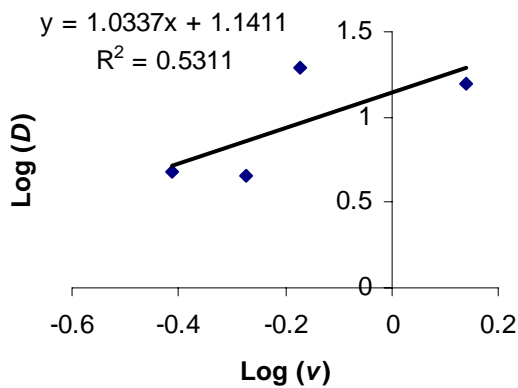


**Fig. 6: Log-Log plots of the dispersion coefficient as a function of the flow velocity, with the fitted linear relationship.**

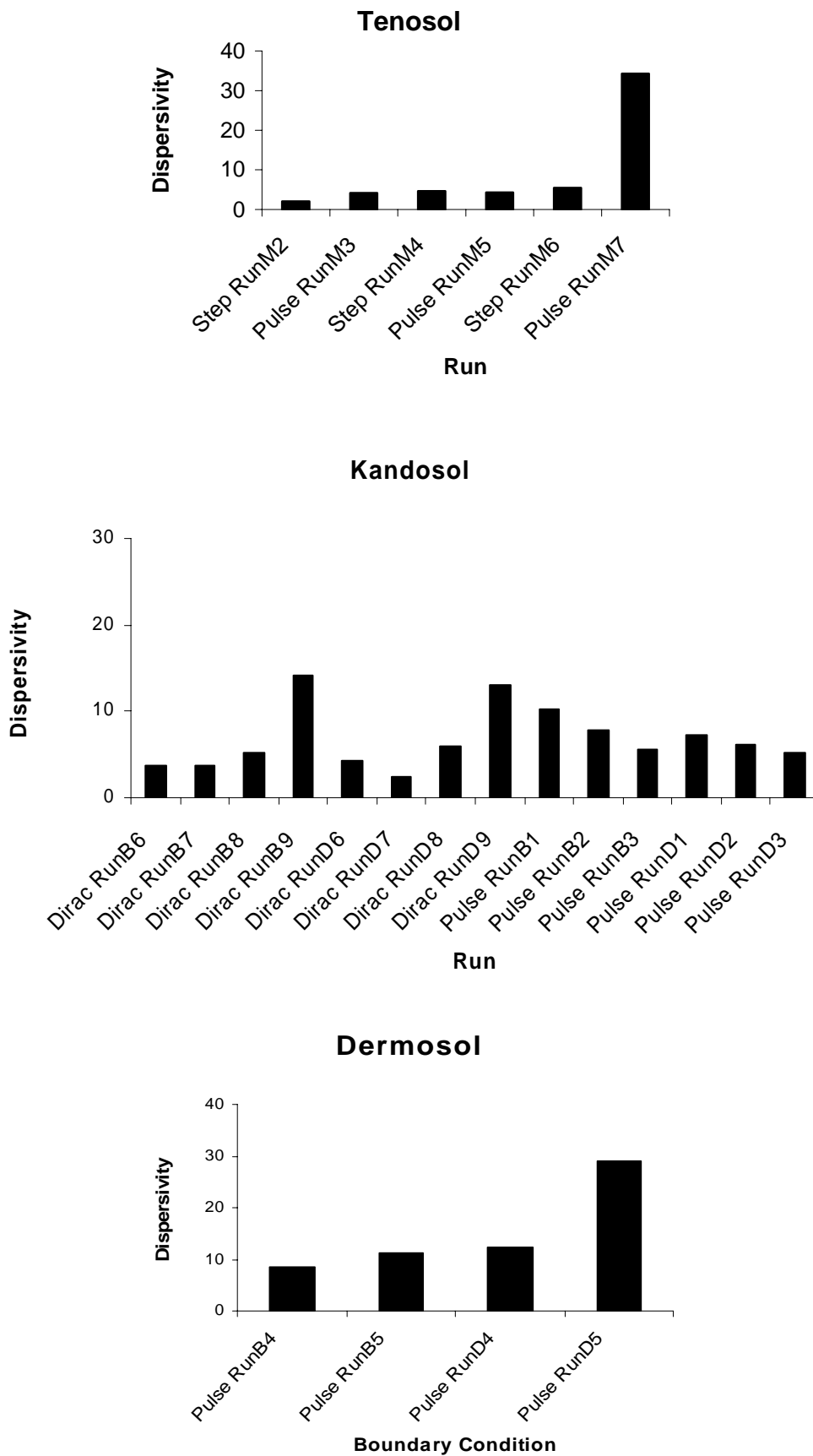


**Fig. 7: Dispersivity  $\varepsilon$  (defined as  $D/v$ ) for each run carried out on the three soils.**